JCTC Journal of Chemical Theory and Computation

Article

pubs.acs.org/JCTC

Tuning Range-Separated Density Functional Theory for Photocatalytic Water Splitting Systems

Olga S. Bokareva, Gilbert Grell, Sergey I. Bokarev,* and Oliver Kühn

Institut für Physik, Universität Rostock, Universitätsplatz 3, D-18055 Rostock, Germany

Supporting Information

ABSTRACT: We discuss the system-specific optimization of long-range-separated density functional theory (DFT) for the prediction of electronic properties relevant for a photocatalytic cycle based on an Ir(III) photosensitizer (IrPS). Special attention is paid to the charge-transfer properties, which are of key importance for the photoexcitation dynamics but cannot be correctly described by means of conventional DFT. The optimization of the range-separation parameter using the ΔSCF method is discussed for IrPS including its derivatives and complexes with electron donors and acceptors used in photocatalytic hydrogen production. Particular attention is paid to the problems arising for a description of medium effects by means of a polarizable continuum model.

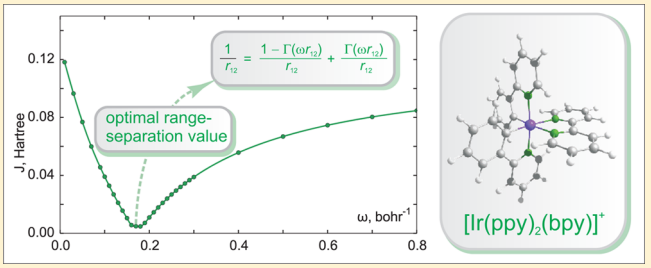

1. INTRODUCTION

Transition metal (TM) organometallic complexes have found use in a wide range of catalytic, medical, and biological applications. In view of the growing demand for energy, one of the most prospective applications of TM complexes is their role in systems for conversion and storage of solar light energy into chemical form. Here, a variety of homogeneous and heterogeneous schemes have been suggested.[1−3] TM complexes are attractive because of their notable spin-orbit coupling. This facilitates the absorption of sunlight, whose energy can be stored in charge-separated triplet states. These long-living triplet states are then available for further reactions. Besides their light-harvesting properties, TM complexes are also used as direct catalysts for water splitting; for recent reviews on homogeneous photocatalysis, see, e.g., refs 4 and 5.

To develop new efficient and stable photocatalytic systems, understanding their primary photoreaction steps and especially excited state properties is required.[6] At the moment, most computationally demanding studies of sizable TM complexes applied in catalysis are performed with DFT in combination with the B3LYP functional and its extension in the time domain in the linear response formulation (TDDFT).[7−15] Besides efficiency, it is the absence of system-dependent parameters that need to be determined first (such as the active space in multireference methods), which makes (TD)DFT attractive. The power of the DFT method to reproduce different electronic ground-state properties even for rather large systems is well-documented.[16] Concerning excited state properties of TM complexes, however, there appears to be no unequivocal opinion; for a review, see ref 17. For an iridium(III) heteroleptic complex, for instance, we have shown that the excited state energies are strongly dependent on the employed exchange-correlation functional.[18] Nevertheless, the TDDFT approach remains the most attractive one.

Many of the practical problems are related to the erroneous description of charge transfer (CT) states.[19,20] To overcome this drawback, different schemes have been proposed, such as, e.g., scaled hybrids[21,22] and range-separated hybrid functionals.[23,24]

Benchmarking DFT results for TM complexes in solution is hampered by the facts that there are no high-resolution experimental data available and only a limited number of theoretical approaches might be applicable to generate a presumably more accurate reference. At the moment, multireference perturbation theory is the best choice for reference calculations of excited state properties. However, in multireference approaches, the problem of a sufficiently large and balanced active space has to be addressed for every system.[18]

In this article, we focus on tuning the range-separation parameter for the long-range-corrected LC-BLYP functional as applied for a particular photocatalytic system developed by Beller et al.[25] It consists of a heteroleptic Ir(III) photosensitizer, triethylamine (TEA) as a sacrificial reductant, and a series of iron carbonyls (Fe-cat) as a water reduction catalyst (Figure 1). In addition, hybrid systems of IrPS and silver nanoparticles are considered.[26−28] Finally, the scope is broadened by including results on modified IrPSs and copper-based PS, which could replace noble-metal containing PS; see ref 29 and references therein. Although the choice of the system is arbitrary, its general properties and the basic reaction steps are common for TM photocatalysis. Therefore, the present study provides some

Received: January 26, 2015

ACS Publications © XXXX American Chemical Society

DOI: 10.1021/acs.jctc.5b00068
J. Chem. Theory Comput. XXXX, XXX, XXX−XXX

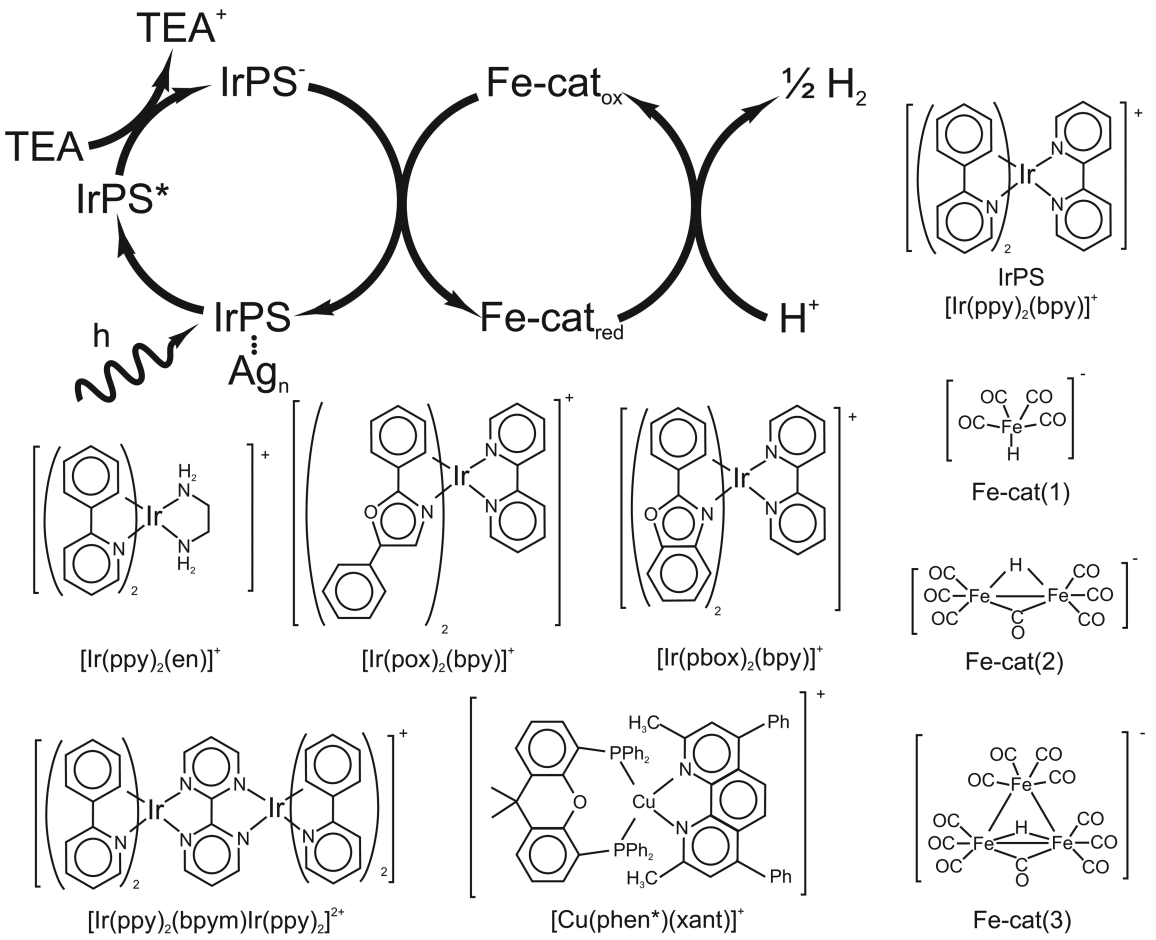

Figure 1. Scheme of photocatalytical water splitting introduced in ref 25 and structural formulas of photosensitizers and water reduction catalysts studied in this work.

general insight into the role of tuning the range-separation parameter in these systems.

In the following section, we start with a brief introduction into the theory of long-range-separated functionals. We then present our results on tuning the range-separation functional for IrPS and joint IrPS-X systems, where X is a reactant responsible for a particular process, i.e., light absorption, electron transfer, and recovery of the ground state. The influence of the reference geometry and environmental and basis set effects are discussed. In particular, the applicability of the ω-tuning together with the polarizable continuum model (PCM) is critically analyzed.

2. OPTIMALLY TUNED RANGE-SEPARATED FUNCTIONALS

DFT has its formal roots in the theorems of Hohenberg and Kohn,[30,31] and it can be considered to be an exact approach, at least in principle. In practice, it is hampered by the lack of the exact exchange correlation (XC) functional, $E_{XC}[\rho(\vec{r})]$, with $\rho(\vec{r})$ being the electron density. There seems to be no first-principle route to $E_{XC}[\rho(\vec{r})]$ and therefore it is usually constructed on the basis of model systems or fitted to experimental reference data. Excited state calculations performed by TDDFT in the linear response approximation employ XC functionals obtained for the electronic ground state.

All caveats and the sometimes spurious behavior of the DFT approach originate from the approximation of the unknown XC kernel. There are three main problems: First, in the $r \to \infty$ limit, the potential and hence the density itself possess an incorrect behavior. In principle, at large distances the potential should be dominated by the exchange term decaying as $-1/r$, whereas the correlation term decays as $\approx -1/r^4$.[32,33] However, for the local density approximation and to a lesser extent for the generalized gradient approximation (GGA), the exchange term decays exponentially.[34] Second, the approximate nature of the exchange term does not cancel the Coulomb interaction of the electron with itself at large r, as is the case for the Hartree−Fock (HF) method (self-interaction error). Third, a well-known deficiency of the approximate Kohn−Sham approach is that the fundamental gap, defined as a difference between the ionization potential (IP) and electron affinity (EA), differs notably from the orbital energy difference $\varepsilon_{HOMO} - \varepsilon_{LUMO}$.[35] This can be explained by the finite jump of the Kohn−Sham correlation potential for a statistical ensemble with variable number of electrons while passing through integer (N) number of electrons, the so-called derivative discontinuity.[35−39] According to Koopmans' theorem for the DFT case,[33,36,40,41] the HOMO corresponds to the IP, but the LUMO is generally more strongly bound than in HF theory and cannot be related to the EA.

Considering TDDFT calculations of electronic excitation energies, the error correlates with the overlap of the donor and acceptor orbitals, being the largest for CT and Rydberg states.[19,20] For vanishing overlap between these orbitals (e.g., due to long-range CT), the excitation energy is reduced to the

DOI: 10.1021/acs.jctc.5b00068
J. Chem. Theory Comput. XXXX, XXX, XXX−XXX

orbital energy difference, being a poor estimate in the case of DFT, which is in contrast to HF theory.

The remedy for the erroneous exchange potential could be the substitution of the approximate density-dependent exchange energy with the exact orbital-dependent one[42] within generalized Kohn−Sham theory.[34,35,42] The exact exchange can be included in a fixed manner, such as in hybrid functionals (e.g., B3LYP), or weighted with a function depending on the interelectron distance r_{12}. The latter case is implemented in range-separated functionals via splitting the Coulomb operator into local and nonlocal parts

$$\frac{1}{r_{12}} = \frac{1 - \Gamma(\omega r_{12})}{r_{12}} + \frac{\Gamma(\omega r_{12})}{r_{12}} \tag{1}$$

where $\Gamma(\omega r_{12})$ is a smooth range-separation function, which damps the exchange contribution from the density functional and complements it with exact exchange. Examples are the Yukawa kernel,[43,44] $e^{-\omega r}/r$, or the error function[24,45] kernel, $\mathrm{erf}(\omega r)/r$. Such an approach eliminates the spurious behavior because the exact exchange has the correct asymptotic character and cancels the asymptotic self-interaction exactly.[46−51]

Certain standard values for the range-separation parameter ω have been established in refs 52 and 53, and they are used like universal constants in popular quantum chemical programs.[54,55] The value 0.33 bohr^{-1} was determined by a least-squares fit to empirical data for first- to third-row atoms[52] and was later refined to 0.47 bohr^{-1} for larger sets of small molecules[53] (for other test sets, see also refs 49, 50, 56, and 57). However, it is clear that for molecules that have not been part of the training sets a more accurate description will be provided by choosing a system-dependent ω. An optimal ω for a particular system can be determined by ensuring that the energy of the HOMO orbital equals the negative of the IP, a relation that would be fulfilled for the exact functional.[58]

However, in the following, we will use an alternative, the so-called ΔSCF method,[49,59,60] where the IP and EA are calculated as the differences between ground-state (gs) energies of systems with N and $N \pm 1$ electrons, i.e.

$$\mathrm{IP}^{\omega}(N) = E^{\omega}_{\mathrm{gs}}(N-1) - E^{\omega}_{\mathrm{gs}}(N) \tag{2}$$

$$\mathrm{IP}^{\omega}(N+1) = \mathrm{EA}^{\omega}(N) = E^{\omega}_{\mathrm{gs}}(N) - E^{\omega}_{\mathrm{gs}}(N+1) \tag{3}$$

This yields the separate tuning conditions

$$J_0(\omega) = |\varepsilon^{\omega}_{\mathrm{HOMO}}(N) + \mathrm{IP}^{\omega}(N)| \tag{4}$$

$$J_1(\omega) = |\varepsilon^{\omega}_{\mathrm{HOMO}}(N+1) + \mathrm{EA}^{\omega}(N)| \tag{5}$$

In order to obtain a proper description of the fundamental gap, the functions $J_0(\omega)$ and $J_1(\omega)$ for IP and EA should be minimized simultaneously. For the present one-parameter formulation, this requires the general function

$$J(\omega) = J_0(\omega) + J_1(\omega) \tag{6}$$

to be minimized. Note that, in general, $J(\omega)$ can be nonzero even for exact functionals because it is defined for systems with different numbers of electrons.

Although minimizing $J(\omega)$ was applied extensively for tuning the range-separation parameter, in ref 61 it was stressed that the ω values are very close to minima of $J_0(\omega)$, eq 4, or $J_1(\omega)$, eq 5, depending on the particular form of the dependencies of $\varepsilon_{\mathrm{HOMO}}$ and the total energy on ω. To avoid such a biased behavior, it was suggested that a least-squares approach should be applied to minimize the resulting error according to[61,62]

$$J^*(\omega) = \sqrt{J_0^2(\omega) + J_1^2(\omega)} \tag{7}$$

Alternatively, for long-range CT systems where donor and acceptor units can be clearly distinguished, ground states of neutral donor and negatively ionized acceptor can be considered in a tuning approach[59,60] based on Mulliken's rule.[63]

It is important to stress that the optimal ω is density and thus system dependent. Thereby, the dependence of ω on the density for range-separated functionals is much more pronounced than that of the scaling factor for hybrid functionals.[34] Since the range-separated functionals eliminate asymptotic self-interaction[46−51,64] and have the correct asymptotic form of nonlocal exact exchange, the correct Coulomb-like behavior of the energy is assured and thus CT and Rydberg excitation energies are improved. Additionally, since the tuned range-separation parameter improves the fundamental gap for the N electron system, one can expect also a better description of electronic excitation energies in TDDFT, where the leading term reads as $\varepsilon_{\mathrm{HOMO}} - \varepsilon_{\mathrm{LUMO}}$.

In the past, it was shown in numerous publications that the optimally tuned functionals indeed improve the description of different molecular properties such as IPs, fundamental and optical gaps, and CT and Rydberg transition energies.[20,35,40,42,50,52,53,59−61,65−83] The accuracy of optimally tuned range-separated functionals was critically tested in ref 61 for basis set variation as well as prediction of relative energies of spin states, binding energies, and the form of potential energy surfaces.

Finally, we note that a generalized form of LC partitioning of the Coulomb interaction proposed by Yanai for CAM-B3LYP[56] is often applied for nonempirical optimal tuning as well (see, e.g., refs 76, 79−82, and 84). Additionally, the simultaneous two-parameter optimization of short- and long-range separation parameters was proposed in order to minimize the delocalization error. Successful applications provided an improved description of molecular properties.[79,80,82]

3. COMPUTATIONAL DETAILS

The tuning of the range-separation parameter ω according to eqs 6 and 7 has been done for the LC-BLYP functional.[45,52,85] It includes the Becke exchange[86] and a correlation part of GGA-type established by Lee, Yang, and Parr.[87,88] This scheme uses eq 1 with an error function kernel as suggested by Hirao et al.[45] For the case of the parent IrPS compound, the results with a tuned ω are compared to those obtained with the standard system-independent values of 0.33 and 0.47 bohr^{-1} as well as with BLYP and B3LYP[89] functionals.

All calculations have been performed using the LANL2DZ ECP basis set for Ir, Fe, Cu, and Ag and the 6-31G(d) basis set for all other atoms. Ref 61 pointed to a strong dependence of the optimal ω on the inclusion of diffuse function for simple atomic and diatomic systems. To test the influence of diffuse basis functions for the present example of IrPS, calculations have been performed with the 6-31+G(d) and 6-31++G(d) basis sets. The inclusion of one or two diffuse function(s) has led to a decrease of ω by 0.01 bohr^{-1}. Since this effect appears to be of minor importance, only results for the 6-31G(d) basis set will be presented.

The impact of reference geometry used for tuning of ω was studied on the example of IrPS. The tuning for the slightly

DOI: 10.1021/acs.jctc.5b00068
J. Chem. Theory Comput. XXXX, XXX, XXX−XXX

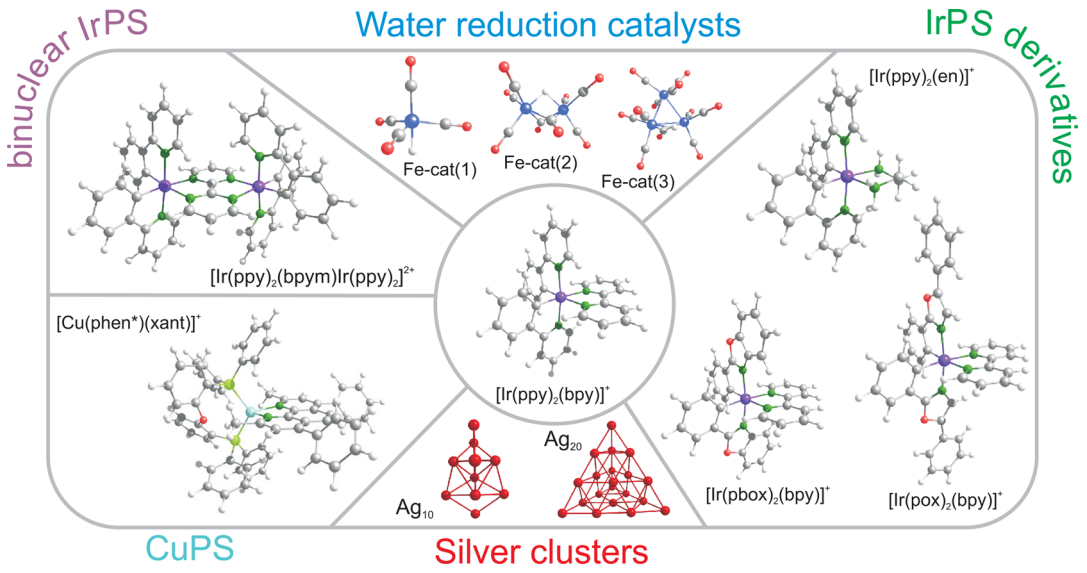

Figure 2. Overview of all optimized structures of those molecules that were used for ω tuning.

different geometries, which have been obtained within LC-BLYP with the two standard (0.33 and 0.47) and the optimized (0.18) ω, led to the same value of 0.18 bohr^{-1}. In the following, the structures optimized with LC-BLYP with optimal ω have been utilized for tuning (Figure 2). For the complexes IrPS-X (X = TEA or Fe-cat), the geometries of the constituing parts have been first optimized separately and then placed at fixed positions without further optimization (for further details, see ref 90). For systems containing silver clusters, the geometries were optimized in refs 26−28. The standard TDDFT formalism was applied for excited state calculations. Solvent effects have been included within the PCM approach.[91] All calculations were done with the Gaussian09 suite of programs.[55]

4. RESULTS AND DISCUSSION

4.1. Optimization of the Range-Separation Parameter. The optimal values of the range-separation parameter ω for molecules and complexes related to the studied photocatalytic system for hydrogen generation (Figure 1) as well as relevant literature data for similar substances are collected in Table 1. In the following, we will discuss particular aspects of the optimization for the chosen target systems.

In the left panel of Figure 3, details of the tuning procedure for the IrPS-Ag$_2$ case are presented. Since $J_0(\omega)$ and $J_1(\omega)$ describe systems with different numbers of electrons, in general, their minima do not coincide. The shown example is the only case among the studied systems in which the minimum of $J(\omega)$ is not well-defined due to an almost flat region from 0.18 to 0.25 bohr^{-1}, where $J_0(\omega)$ and $J_1(\omega)$, upon summation, compensate each other. If the least-squares function $J^*(\omega)$ is applied instead, then a minimum at 0.19 bohr^{-1} can be easily located. For all other test systems collected in Table 1, the minima of J and J^* were very close to each other; J^* led, in some cases, to a decrease of ω by 0.01−0.02 bohr^{-1}. Since the use of J^* was not crucial in our case, we focused on the results obtained by applying J, as it was the main approach of previous investigations.

In the right panel of Figure 3, selected examples of $J(\omega)$ for IrPS in different environments are presented. The curve for IrPS(vac) represents a case with regular behavior, i.e., there is a distinct minimum. For IrPS-Ag$_{10}$, the region after 0.25 bohr^{-1} corresponds to a changed order of HOMO and HOMO − 1 orbitals for the N + 1 electron system. For the isolated reduced

Table 1. Optimized Range-Separation Parameters, ω, Defined by the Minumum of $J(\omega)$, eq 6, for Different Molecules Depicted in Figure 1[a]

compound	optimal ω (bohr^{-1})
IrPS	0.18
IrPS (THF, PCM)	0.05
IrPS + 28 THF	0.15
[Ir(ppy)2(en)]$^+$	0.18
[Ir(pox)2(bpy)]$^+$	0.18
[Ir(pbox)2(bpy)]$^+$	0.18
[Ir(ppy)2(bpym)Ir(ppy)2]$^+$	0.14
[Cu(phen*)(xant)]$^+$	0.16
Ag2	0.42
Ag10	0.22
Ag20	≈0.20[b]
IrPS-Ag$_2$	0.18−0.25[c]
IrPS-Ag$_{10}$	0.16
IrPS-Ag$_{20}$	0.16
TEA	0.31
IrPS-TEA	0.23−0.32[d]
Fe-cat(1)	0.24
Fe-cat(2)	0.19
Fe-cat(3)	0.17
IrPS-Fe-cat(1)	0.18[d]
IrPS-Fe-cat(2)	0.17−0.18[d]
IrPS-Fe-cat(3)	0.16−0.17[d]
C_{60}[70]	0.21
phthalocyanine[70]	0.16
Si-nanocrystals (5−15 Å)[69]	0.10−0.24
coumarine dyes[60]	0.17−0.21
pentacene-C_{60}[81]	0.21
nucleobases[78]	0.27−0.31

[a]For comparison, literature data on molecules relevant for photovoltaics are provided. [b]Because of convergence problems, only a tentative value is given. [c]Using $J(\omega)$, eq 6, a flat dependence is obtained; see the text and Figure 3. [d]Different geometries are used; see the text.

DOI: 10.1021/acs.jctc.5b00068
J. Chem. Theory Comput. XXXX, XXX, XXX−XXX

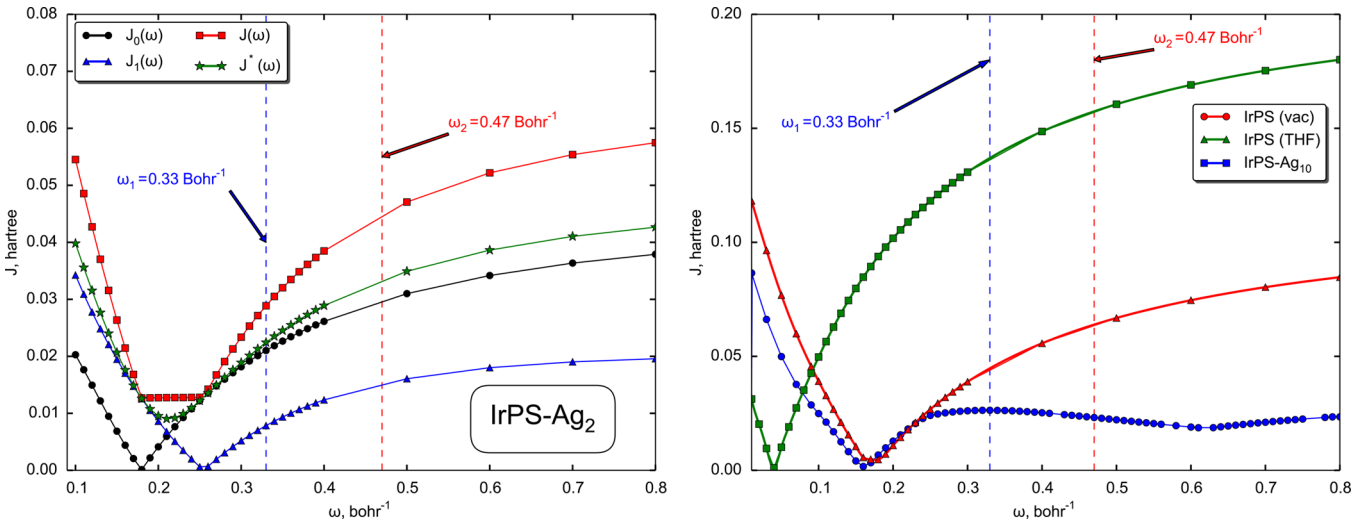

Figure 3. (Left) Functions defined in eqs 4−7 used for optimization of the range-separation parameter ω for IrPS-Ag_2. (Right) Selected examples of $J(\omega)$ for IrPS in different environments.

IrPS in the doublet electronic state, the unpaired electron was previously shown to be localized on the π(bpy)* orbital.[92] For IrPS-Ag_{10}, an internal oxidation−reduction occurs for $\omega > 0.25$ bohr^{-1}: the unpaired electron moves from π(bpy)* to σ* (Ag).

As IrPS forms no stable complexes, IrPS-X, neither with TEA nor with the iron catalysts,[90] the relative position of constituents might be flexibly varied. Similar to the procedure in ref 90, we have varied the position of X = TEA or Fe-cat on a sphere around IrPS. Thereby, we found that choosing different locations does not have an impact on the resulting ω. However, changing the distance between IrPS and X led to some variation of the optimal ω (Table 1). Interestingly, the optimal ω value was found to increase in the range 0.23−0.32 bohr^{-1} with increasing distance between IrPS and TEA from 7 to 12 Å. While the minimal value of $J_0(\omega)$ remains at 0.18 bohr^{-1}, the minimum of $J_1(\omega)$ occurs at larger ω. The usage of $J^*(\omega)$ instead of $J(\omega)$ provides a narrower range of 0.23−0.28 bohr^{-1}. We note that in refs 49 and 61 it was shown that an optimization of ω for each geometry and subsystem can lead to size inconsistency or unphysical potential energy curves in excited states.

For comparison, the standard[52,53] system-independent ω_1 =0.33 bohr^{-1} and ω_2 =0.47 bohr^{-1} are shown in both panels of Figure 3 by vertical lines. As can be seen from that figure and Table 1, the optimally tuned ω values for compounds relevant in photocatalysis are substantially lower than those determined for diatomics and small molecules.[52,53] Since ω^{-1} reflects a characteristic distance for switching between short- and long-range parts or, in other words, an effective electron screening (delocalization) length, previously optimal ω values were found to decrease with increasing system size and conjugation length.[60,69,70,72,73,77,93] However, in some cases, the dependence was not monotonous and strongly varied for systems with different electronic structure.[70] In the present study, the Ir(III) complexes have various sizes, being smallest for $[Ir(ppy)_2(en)]^+$ and largest for $[Ir(ppy)_2(bpym)\ Ir(ppy)_2]^+$. However, only a minor dependence of ω on the size of ligands around the central Ir atom and the size of molecules (silver clusters, iron carbonyls) bound to the PS was found (cf. Table 1).

4.2. Effect of Solvation. By requiring Koopmans' theorem to be satisfied simultaneously for systems with N and $N + 1$ electrons where HOMO and LUMO are on different fragments, we automatically improve the description of electron transfer. This implies that the long-range-corrected functional with an optimized range-separation parameter should have a predictive power to study redox properties. To describe redox (electron transfer) reactions in photocatalysis, solvent effects need to be included. However, ω tuning in the presence of a solvent was only rarely addressed.[94−97] In ref 94, solvent effects on CT states energies were included by a charge-constraint DFT approach on top of vacuum-optimized ω. In ref 96, solvent shifts of ionization energies for photovoltaic materials have been analyzed via PCM ΔSCF calculations using an ω that was tuned for the vacuum case. In ref 95, the tuning procedure was generalized to the crystal phase by accounting for dielectric screening effects. The only work on the optimal tuning in PCM solvent for a series of oligothiophenes was published recently.[97]

In the following, we focus on the combination of optimal tuning with the PCM model for selected examples. The green curve with square symbols in Figure 3 shows $J(\omega)$ for IrPS, solvated via the PCM model (THF solvent). This yields a very small optimal ω = 0.05 bohr^{-1}. Similar computations have been done for TEA and Fe-cat(3), resulting in values 0.10 and 0.05 bohr^{-1}, respectively. Note that such a small value of ω implies that there is almost no long-range correction from exact HF exchange. Interestingly, the inclusion of 28 explicit THF molecules around IrPS, which corresponds to one solvation shell, led to ω = 0.15 bohr^{-1}, similar to the vacuum case. This means that the increasing system size through explicit inclusion of the first solvation shell has only a minor impact on the value of optimal range separation parameter.

In Figure 4, the dependencies of IPs and HOMO orbital energies on the ω are presented for the vacuum and PCM cases for IrPS with N and $N + 1$ electrons. The crossing points between corresponding IP and HOMO lines mark the optimal ω according to the tuning conditions (eqs 4 and 5). In ref 97, the HOMO energies of oligothiophenes were shown to have almost the same dependence on ω with and without solvent. Therefore, the unrealistic lowering of ω was attributed to the underestimation of vertical IPs in the ΔSCF procedure with equilibrium solvation. The situation becomes more involved in the case of IrPS, where, for reduced species (Figure 4, right), the difference between vacuum and solvent is indeed mostly

DOI: 10.1021/acs.jctc.5b00068
J. Chem. Theory Comput. XXXX, XXX, XXX−XXX

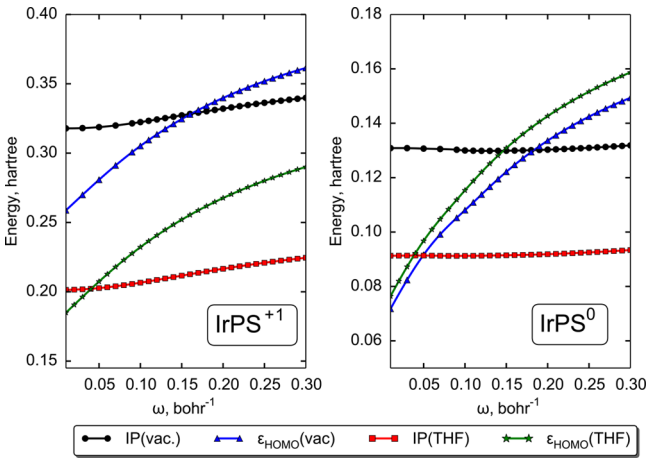

Figure 4. Dependencies of IP and negative of $\varepsilon(\omega)$ for IrPS in vacuum and THF on the range-separation parameter ω. Right, oxidized IrPS; left, reduced IrPS.

due to the IP, but for the oxidized species (Figure 4, left), orbital energies depend on the inclusion of solvent as well. Hence, the lowering of the optimal ω cannot be attributed solely to the erroneous description of the IP.

According to Janak's theorem,[98] the redox energy upon changing the number of electrons from $N-1$ to N can be obtained in integral form as

$$\Delta E = \int_{N-1}^{N} \varepsilon_{\mathrm{orb}}(n)\, \mathrm{d}n \tag{8}$$

In the absence of self-interaction and delocalization errors, the orbital energies $\varepsilon_{\mathrm{orb}}$ stay constant between integer numbers of electrons, thus satisfying the conditions of ω optimization, eq 2. In Figure 5, redox and HOMO/LUMO energies are shown for different functionals and optimization conditions. For the tuned ω, $\Delta E = -\varepsilon_{\mathrm{HOMO}}(N) = -\varepsilon_{\mathrm{LUMO}}(N-1)$ are given in the central panel of Figure 4 for IrPS in vacuum. When using the conventional BLYP functional, this condition is not satisfied (left panel). However, if we include implicit PCM solvation, then the jump in energies of HOMO(N) and LUMO($N-1$) is mitigated by the response of the polarizable continuum. This leads to much better estimates of redox energies obtained with conventional functionals with PCM as compared with vacuum.[99] In other words, in terms of the derivative discontinuity, the PCM solvent effectively leads to a partial mitigation of the E_{XC} deficiencies.

That is why one needs to include much less exact exchange into the LC-BLYP functional (smaller ω) to satisfy Koopmans' theorem and the derivative discontinuity condition, as is seen from Figure 3 and Table 1. The orbital eigenvalues in the right panel of Figure 5 for the solvent case are almost constant, with the deviations probably being due to a residual delocalization error. Importantly, the ω value optimized for the vacuum does not fulfill the condition of constant orbital energies in solvent and vice versa. Further examples of Fe-cat(3) and TEA leading to the same conclusion can be found in the Supporting Information.

4.3. Triplet Stability. The nature and energetic position of the lowest triplet state of PSs need to be calculated very accurately since this state plays a key role in photoprocesses as a dominant long-living and emitting excited state. However, the calculation of triplet states represents a challenge for the TDDFT approach with long-range corrected hybrid functionals because of symmetry breaking instabilities of the ground-state solution.[100,101] Typically, the larger amount of exact exchange leads to more pronounced problems with instabilities of the ground-state wave function. This results in a divergence of TDDFT excitation energies and an imaginary energy of the lowest triplet state.[102] As shown in ref 72, the nonempirical tuning of ω could avoid the instabilities through the stabilizing the ground-state solution, but this issue should be carefully analyzed for the particular system under study. Since the instability problems are generally more pronounced for the HF

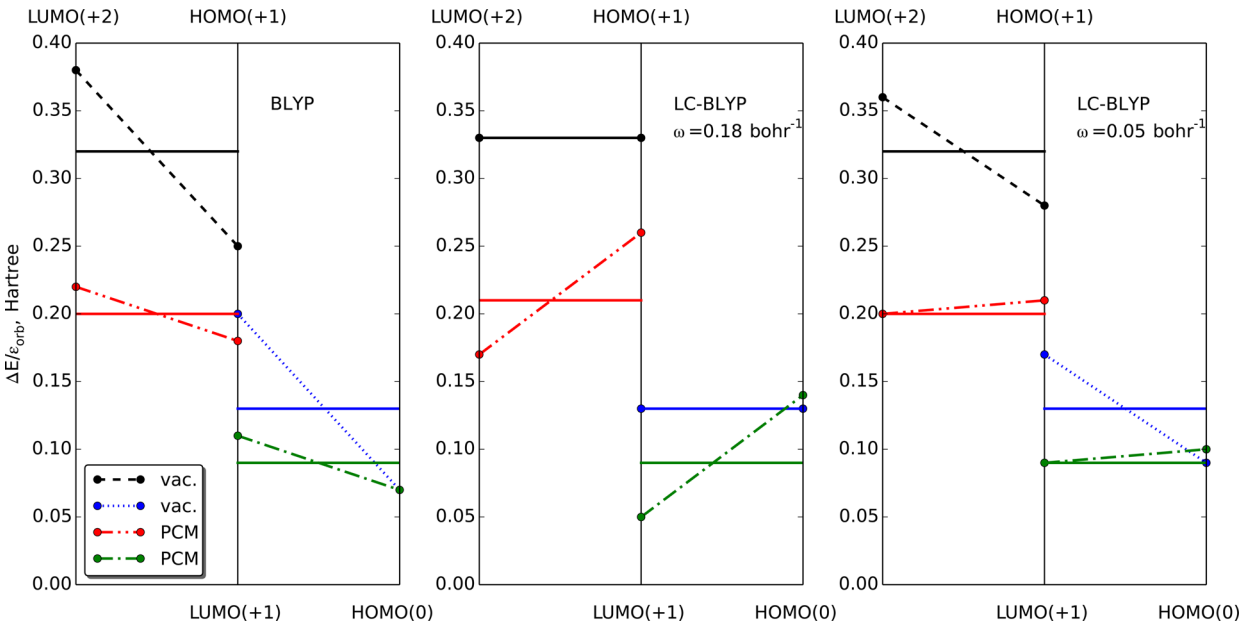

Figure 5. ΔSCF redox energies ΔE (dashed lines) and orbital eigenvalues $-\varepsilon_{\mathrm{HOMO/LUMO}}$(solid lines) for different charge states (+2,+1, and 0) of IrPS computed with pure BLYP and LC-BLYP with ω optimization in vacuum and PCM solvent. The eigenvalue of the β spin-orbital was used for LUMO(+2); all other values correspond to the α spin-orbital.

DOI: 10.1021/acs.jctc.5b00068
J. Chem. Theory Comput. XXXX, XXX, XXX−XXX

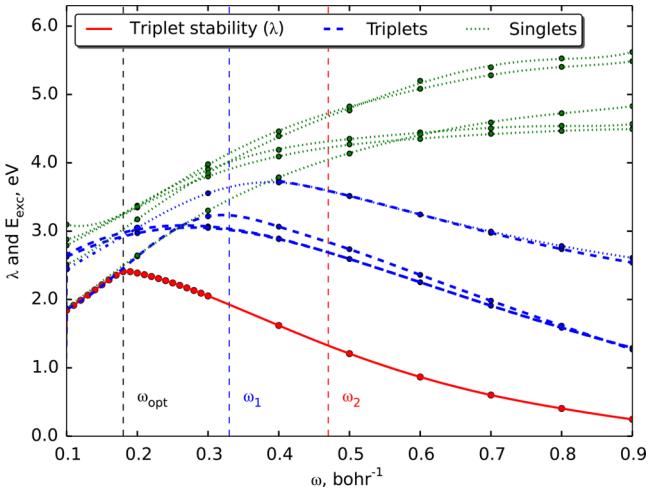

Figure 6. Energies of the lowest five singlet and triplet excited states and the lowest eigenvalue of the ground-state stability matrix (λ) in dependence on the range-separation parameter ω for IrPS in vacuum.

method than for DFT,[72,100] the application of a smaller value for ω should result in a more stable ground-state solution. In Figure 6, the dependence of the smallest eigenvalue of the triplet stability matrix[100] on the range-separation parameter, $\lambda(\omega)$, for the case of IrPS is given; the energies of the lowest triplet and singlet energies are provided as well.

It can be clearly seen that for the present system the maximum stability λ_{max} corresponds to the optimal ω value. The λ value is notably higher for the standard values $\omega_{1,2}$.[52,53] This implies that LC-BLYP with a properly tuned range-separation parameter ensures a more reliable estimate of triplet state energies. The singlet state energies systematically rise with the increase of the exact exchange part, which is a common behavior for TDDFT.[18] For triplet states, this rising is compensated by the decrease in energy upon the increase of instability, resulting in maxima around 0.25−0.40 bohr^{-1}.

4.4. Electronic Absorption Spectra. A comparative analysis of excitation and differential absorption spectra of IrPS in THF calculated by means of local (BLYP), hybrid (B3LYP), and long-range corrected LC-BLYP with standard and both optimal (for vacuum and THF) ω values is provided in Figure 7. In the TDDFT calculations, the 80 lowest singlet−singlet states have been included and assigned. A phenomenological broadening by a Gaussian line shape with a width of 0.1 eV was assumed.

Overall, the features of the absorption spectrum are well-reproduced by B3LYP and LC-BLYP with optimal ω = 0.18 bohr^{-1}. However, absorption and difference spectra could only be properly assigned simultaneously using LC-BLYP (ω = 0.18 bohr^{-1}).[92] It should be noted that besides the overall shape of spectra, which can be described by the conventional hybrid functional, the quality of the description of CT states and band gap characteristics is only assured for the long-range functional with the properly tuned ω parameter. The excessive amount of HF exchange (as in LC-BLYP with both standard ω values) as well as complete absence of exact exchange (as in BLYP) led to shapes of absorption and difference spectra of IrPS deviating from experiments. Naturally, the results of LC-BLYP with optimal ω tuned for PCM are very close to those of pure BLYP because only a small amount of exact exchange is included. Hence, LC-BLYP with ω = 0.05 bohr^{-1} optimized in a PCM solvent model does not agree with experiment, similar to the parent BLYP functional, which is known for wrongly predicting energies of CT states.

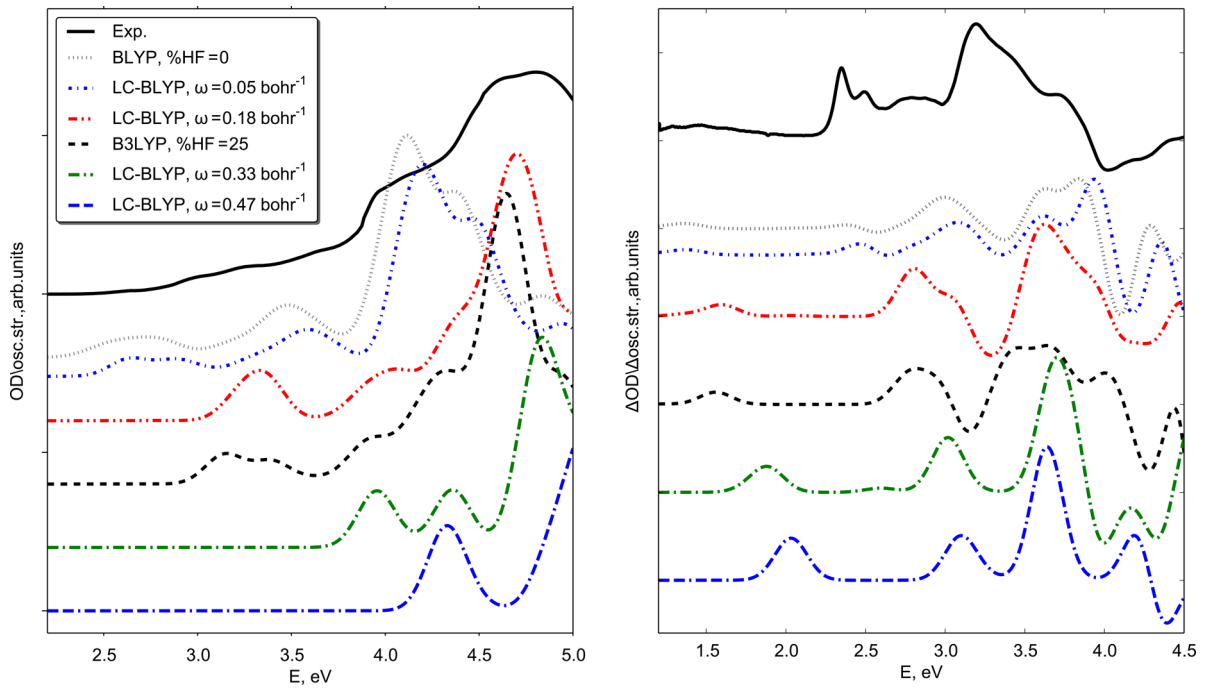

Figure 7. (Left) Experimental (optical density, OD) and theoretical (TDDFT, oscillator strength) electronic excitation spectra. (Right) Difference absorption spectra (reduced species − oxidized species) obtained theoretically and by transient absorption experiments of IrPS in THF solution. Experimental spectra were measured by Lochbrunner et al. and had been published together with the calculated BLYP and B3LYP spectra in refs 18 and 92. All calculations included THF within the PCM.

DOI: 10.1021/acs.jctc.5b00068
J. Chem. Theory Comput. XXXX, XXX, XXX−XXX

The latter observation deserves additional comments. In view of the derivative discontinuity, $\omega = 0.05$ bohr^{-1} obtained for the PCM model gives an improved description as compared to the gas-phase value (Figure 5, right). In contrast, using the gas phase $\omega = 0.18$ bohr^{-1} together with a PCM model yields overscreening (Figure 5, middle). At this point, one should note that under the influence of a polar solvent the energies of CT and local states shift differently from their vacuum values because of substantially different dipole moments. That is why, to correctly predict the electronic absorption spectrum in solution, one needs to use ω tuned in vacuum and to include solvent effects via PCM. In other words, we observe that, when using the PCM model, for obtaining a reasonable agreement between measured and calculated absorption spectra one has to sacrifice the derivative discontinuity condition.

5. CONCLUSIONS

The present investigation of molecules and complexes relevant to photochemical water splitting points to the need for a system-specific optimization of the range-separation parameter within the LC-BLYP approach. It provides improved band gap characteristics, increased ground-state stability, and a correct asymptotic behavior of CT states. The actual optimized value, $\omega = 0.18$ bohr^{-1}, was found to be nearly the same for various Ir- and Cu-based PS as well as for IrPS complexes with silver clusters and iron carbonyls. Using ω optimization, it was shown that the tuning for supermolecular compound systems, where an electron relay between constituents is of interest, gives an improvement of the energies of HOMO and LUMO orbitals localized on different fragments. Thus, this approach is, in principle, suitable for accurate modeling of redox molecular properties.

The optimization of the range-separation parameter is usually performed for molecules in vacuum. In the present article, we discussed the inclusion of solvent, introduced by the PCM, for selected cases. For the used ΔSCF approach, the optimal ω tends to zero, in accordance with recent results for oligothiophenes.[97] As a consequence, there is almost no long-range correction and the quality, e.g., of electronic excitation spectra, corresponds to that of the BLYP functional. Since CT and long-range properties are of primary interest for photocatalysis, it is recommended to use ω optimized in vacuum together with PCM. This seems to provide a better description of CT processes and electronic absorption spectra, even though the formal conditions imposed by the derivative discontinuity are violated. Therefore, if redox reactions are studied, the combination ΔSCF/PCM is not recommended. It either leads to derivative discontinuity problems or to a wrong asymptotic behavior of the optimized functional. Needless to say, this procedure should not be applied without careful diagnostics, e.g., as provided by Figure 5.

■ ASSOCIATED CONTENT

Supporting Information

Full data on ΔSCF redox energies and orbital eigenvalues for IrPS, TEA, and Fe-cat(3). This material is available free of charge via the Internet at http://pubs.acs.org.

■ AUTHOR INFORMATION

Corresponding Author

*E-mail: sergey.bokarev@uni-rostock.de.

Funding

This work has been supported by the BMBF within the project "Light2Hydrogen" (Spitzenforschung und Innovation in den Neuen Ländern), by the European Union (European Social Funds, ESF) within the project "PS4H" and by the Ministry for Education, Science and Culture of Mecklenburg-Vorpommern.

Notes

The authors declare no competing financial interest.

■ REFERENCES

(1) Esswein, A. J.; Nocera, D. G. *Chem. Rev.* **2007**, *107*, 4022−47.
(2) Hambourger, M.; Moore, G. F.; Kramer, D. M.; Gust, D.; Moore, A. L.; Moore, T. A. *Chem. Soc. Rev.* **2009**, *38*, 25−35.
(3) Blankenship, R. E.; Tiede, D. M.; Barber, J.; Brudvig, G. W.; Fleming, G.; Ghirardi, M.; Gunner, M. R.; Junge, W.; Kramer, D. M.; Melis, A.; Moore, T. A.; Moser, C. C.; Nocera, D. G.; Nozik, A. J.; Ort, D. R.; Parson, W. W.; Prince, R. C.; Sayre, R. T. *Science* **2011**, *332*, 805−9.
(4) Hagfeldt, A.; Boschloo, G.; Sun, L.; Kloo, L.; Pettersson, H. *Chem. Rev.* **2010**, *110*, 6595−663.
(5) Eckenhoff, W. T.; Eisenberg, R. *Dalton Trans.* **2012**, *41*, 13004−21.
(6) You, Y.; Nam, W. *Chem. Soc. Rev.* **2012**, *41*, 7061−84.
(7) Tinker, L. L.; McDaniel, N. D.; Curtin, P. N.; Smith, C. K.; Ireland, M. J.; Bernhard, S. *Chemistry* **2007**, *13*, 8726−32.
(8) Li, X.-N.; Wu, Z.-J.; Zhang, H.-J.; Liu, X.-J.; Zhou, L.; Li, Z.-F.; Si, Z.-J. *Phys. Chem. Chem. Phys.* **2009**, *11*, 6051−6059.
(9) Costa, R. D.; Viruela, P. M.; Bolinka, H. J.; Ortí, E. *J. Mol. Struct.* **2009**, *912*, 21−26.
(10) Tian, N.; Lenkeit, D.; Pelz, S.; Fischer, L. H.; Escudero, D.; Schiewek, R.; Klink, D.; Schmitz, O. J.; González, L.; Schäferling, M.; Holder, E. *Eur. J. Inorg. Chem.* **2010**, 4875−4885.
(11) Ladouceur, S.; Fortin, D.; Zysman-Colman, E. *Inorg. Chem.* **2010**, *49*, 5625−5641.
(12) Wu, S.-H.; Ling, J.-W.; Lai, S.-H.; Huang, M.-J.; Cheng, C. H.; Chen, I.-C. *J. Phys. Chem. A* **2010**, *114*, 10339−10344.
(13) Takizawa, S.-y.; Shimada, K.; Sato, Y.; Murata, S. *Inorg. Chem.* **2014**, *53*, 2983−95.
(14) Chirdon, D. N.; Transue, W. J.; Kagalwala, H. N.; Kaur, A.; Maurer, A. B.; Pintauer, T.; Bernhard, S. *Inorg. Chem.* **2014**, *53*, 1487−99.
(15) Song, M.-X.; Wang, G.-F.; Wang, J.; Wang, Y.-H.; Bai, F.-Q.; Qin, Z.-K. *Spectrochim. Acta, Part A* **2014**, *134C*, 406−412.
(16) Sousa, S. F.; Fernandes, P. A.; Ramos, M. J. *J. Phys. Chem. A* **2007**, *111*, 10439−10452.
(17) Laurent, A. D.; Jacquemin, D. *J. Int. Quantum Chem.* **2013**, *113*, 2019−2039.
(18) Bokarev, S. I.; Bokareva, O. S.; Kühn, O. *J. Chem. Phys.* **2012**, *136*, 214305.
(19) Dreuw, A.; Head-Gordon, M. *Chem. Rev.* **2005**, *105*, 4009−4037.
(20) Peach, M. J. G.; Benfield, P.; Helgaker, T.; Tozer, D. J. *J. Chem. Phys.* **2008**, *128*, 44118.
(21) Becke, A. D. *J. Chem. Phys.* **1993**, *98*, 1372.
(22) Adamo, C.; Barone, V. *J. Chem. Phys.* **1998**, *108*, 664.
(23) Savin, A. In *Recent Advances in Computational Chemistry*; Chong, D. P., Ed.; World Scientific: Hoboken, NJ, 1995; Vol. *1*, pp 129−153.
(24) Leininger, T.; Stoll, H.; Werner, H.-J.; Savin, A. *Chem. Phys. Lett.* **1997**, *275*, 151−160.
(25) Gärtner, F.; Sundararaju, B.; Surkus, A.-E.; Boddien, A.; Loges, B.; Junge, H.; Dixneuf, P. H.; Beller, M. *Angew. Chem., Int. Ed.* **2009**, *48*, 9962.
(26) Bokareva, O. S.; Bokarev, S. I.; Kühn, O. *Phys. Chem. Chem. Phys.* **2012**, *14*, 4977−84.
(27) Bokareva, O. S.; Kühn, O. *Chem. Phys.* **2014**, *435*, 40−48.
(28) Bokareva, O. S.; Kühn, O. *arXiv.org, e-Print Arch., Phys.* **2015**, arXiv:1501.04492.

DOI: 10.1021/acs.jctc.5b00068
J. Chem. Theory Comput. XXXX, XXX, XXX−XXX

(29) Fischer, S.; Hollmann, D.; Tschierlei, S.; Karnahl, M.; Rockstroh, N.; Barsch, E.; Schwarzbach, P.; Luo, S.-p.; Junge, H.; Beller, M.; Lochbrunner, S.; Ludwig, R.; Brückner, A. *ACS Catal.* **2014**, *4*, 1845−1849.
(30) Hohenberg, P.; Kohn, W. *Phys. Rev.* **1964**, *136*, B864−B871.
(31) Kohn, W.; Sham, L. J. *Phys. Rev.* **1965**, *140*, A1133−A1138.
(32) Handy, N.; Marron, M.; Silverstone, H. *Phys. Rev.* **1969**, *180*, 45−48.
(33) Almbladh, C.-O.; von Barth, U. *Phys. Rev. B* **1985**, *31*, 3231−3244.
(34) Baer, R.; Livshits, E.; Salzner, U. *Annu. Rev. Phys. Chem.* **2010**, *61*, 85−109.
(35) Kronik, S.; Kümmel, L. *Rev. Mod. Phys.* **2008**, *80*, 3−60.
(36) Perdew, J. P.; Levy, M.; Balduz, J. L. *Phys. Rev. Lett.* **1982**, *49*, 1691−1694.
(37) Sham, L.; Schlüter, M. *Phys. Rev. Lett.* **1983**, *51*, 1888−1891.
(38) Godby, R.; Schlüter, M.; Sham, L. *Phys. Rev. Lett.* **1986**, *56*, 2415−2418.
(39) Allen, M. J.; Tozer, D. J. *Mol. Phys.* **2002**, *100*, 433−439.
(40) Cohen, A.; Mori-Sánchez, P.; Yang, W. *Phys. Rev. B* **2008**, *77*, 115123.
(41) Salzner, U.; Baer, R. *J. Chem. Phys.* **2009**, *131*, 231101.
(42) Seidl, A.; Görling, A.; Vogl, P.; Majewski, J.; Levy, M. *Phys. Rev. B* **1996**, *53*, 3764−3774.
(43) Baer, R.; Neuhauser, D. *Phys. Rev. Lett.* **2005**, *94*, 043002.
(44) Akinaga, Y.; Ten-no, S. *Chem. Phys. Lett.* **2008**, *462*, 348−351.
(45) Iikura, H.; Tsuneda, T.; Yanai, T.; Hirao, K. *J. Chem. Phys.* **2001**, *115*, 3540−3544.
(46) Gerber, I. C.; Ángyán, J. G. *Chem. Phys. Lett.* **2005**, *415*, 100−105.
(47) Zhao, Y.; Truhlar, D. G. *J. Phys. Chem. A* **2006**, *110*, 13126−30.
(48) Peach, M. J. G.; Helgaker, T.; Salek, P.; Keal, T. W.; Lutnaes, O. B.; Tozer, D. J.; Handy, N. C. *Phys. Chem. Chem. Phys.* **2006**, *8*, 558−62.
(49) Livshits, E.; Baer, R. *Phys. Chem. Chem. Phys.* **2007**, *9*, 2932−2941.
(50) Chai, J.-D.; Head-Gordon, M. *J. Chem. Phys.* **2008**, *128*, 084106.
(51) Mori-Sánchez, P.; Cohen, A. J.; Yang, W. *J. Chem. Phys.* **2006**, *124*, 91102.
(52) Tawada, Y.; Tsuneda, T.; Yanagisawa, S.; Yanai, T.; Hirao, K. *J. Chem. Phys.* **2004**, *120*, 8425−8433.
(53) Song, J.-W.; Hirosawa, T.; Tsuneda, T.; Hirao, K. *J. Chem. Phys.* **2007**, *126*, 154105.
(54) Schmidt, M. W.; Baldridge, K. K.; Boatz, J. A.; Elbert, S. T.; Gordon, M. S.; Jensen, J. H.; Koseki, S.; Matsunaga, N.; Nguyen, K. A.; Su, S.; Windus, T. L.; Dupuis, M.; Montgomery, J. A., Jr. *J. Comput. Chem.* **1993**, *14*, 1347−1363.
(55) Frisch, M. J.; Trucks, G. W.; Schlegel, H. B.; Scuseria, G. E.; Robb, M. A.; Cheeseman, J. R.; Scalmani, G.; Barone, V.; Mennucci, B.; Petersson, G. A.; Nakatsuji, H.; Caricato, M.; Li, X.; Hratchian, H. P.; Izmaylov, A. F.; Bloino, J.; Zheng, G.; Sonnenberg, J. L.; Hada, M.; Ehara, M.; Toyota, K.; Fukuda, R.; Hasegawa, J.; Ishida, M.; Nakajima, T.; Honda, Y.; Kitao, O.; Nakai, H.; Vreven, T.; Montgomery, J. A., Jr.; Peralta, J. E.; Ogliaro, F.; Bearpark, M.; Heyd, J. J.; Brothers, E.; Kudin, K. N.; Staroverov, V. N.; Kobayashi, R.; Normand, J.; Raghavachari, K.; Rendell, A.; Burant, J. C.; Iyengar, S. S.; Tomasi, J.; Cossi, M.; Rega, N.; Millam, J. M.; Klene, M.; Knox, J. E.; Cross, J. B.; Bakken, V.; Adamo, C.; Jaramillo, J.; Gomperts, R.; Stratmann, R. E.; Yazyev, O.; Austin, A. J.; Cammi, R.; Pomelli, C.; Ochterski, J. W.; Martin, R. L.; Morokuma, K.; Zakrzewski, V. G.; Voth, G. A.; Salvador, P.; Dannenberg, J. J.; Dapprich, S.; Daniels, A. D.; Farkas, O.; Foresman, J. B.; Ortiz, J. V.; Cioslowski, J.; Fox, D. J. *Gaussian 09*, revision C.1; Gaussian, Inc.: Wallingford, CT, 2009.
(56) Yanai, T.; Tew, D. P.; Handy, N. C. *Chem. Phys. Lett.* **2004**, *393*, 51−57.
(57) Rohrdanz, M. A.; Martins, K. M.; Herbert, J. M. *J. Chem. Phys.* **2009**, *130*, 054112.
(58) Perdew, J.; Levy, M. *Phys. Rev. B* **1997**, *56*, 16021−16028.
(59) Stein, T.; Kronik, L.; Baer, R. *J. Am. Chem. Soc.* **2009**, *131*, 2818−2820.
(60) Stein, T.; Kronik, L.; Baer, R. *J. Chem. Phys.* **2009**, *131*, 244119.
(61) Karolewski, A.; Kronik, L.; Kümmel, S. *J. Chem. Phys.* **2013**, *138*, 204115.
(62) Kronik, L.; Stein, T.; Refaely-Abramson, S.; Baer, R. *J. Chem. Theory Comput.* **2012**, *8*, 1515−1531.
(63) Mulliken, R. S. *J. Am. Chem. Soc.* **1950**, *72*, 600−608.
(64) Vydrov, O. A.; Scuseria, G. E. *J. Chem. Phys.* **2006**, *125*, 234109.
(65) Sekino, H.; Maeda, Y.; Kamiya, M.; Hirao, K. *J. Chem. Phys.* **2007**, *126*, 014107.
(66) Lange, A. W.; Rohrdanz, M. A.; Herbert, J. M. *J. Phys. Chem. B* **2008**, *112*, 7345−7345.
(67) Lange, A. W.; Rohrdanz, M. A.; Herbert, J. M. *J. Phys. Chem. B* **2008**, *112*, 6304−6308.
(68) Akinaga, Y.; Ten-no, S. *Int. J. Quantum Chem.* **2009**, *109*, 1905−1914.
(69) Stein, T.; Eisenberg, H.; Kronik, L.; Baer, R. *Phys. Rev. Lett.* **2010**, *105*, 266802.
(70) Refaely-Abramson, S.; Baer, R.; Kronik, L. *Phys. Rev. B* **2011**, *84*, 075144.
(71) Wong, B. M.; Piacenza, M.; Della Sala, F. *Phys. Chem. Chem. Phys.* **2009**, *11*, 4498−4508.
(72) Sears, J. S.; Körzdörfer, T.; Zhang, C.-R.; Brédas, J.-L. *J. Chem. Phys.* **2011**, *135*, 151103.
(73) Körzdörfer, T.; Sears, J. S.; Sutton, C.; Brédas, J.-L. *J. Chem. Phys.* **2011**, *135*, 204107.
(74) Kuritz, N.; Stein, T.; Baer, R.; Kronik, L. *J. Chem. Theory Comput.* **2011**, *7*, 2408−2415.
(75) Moore, B.; Autschbach, J. *ChemistryOpen* **2012**, *1*, 184−194.
(76) Egger, D. A.; Weissman, S.; Refaely-Abramson, S.; Sharifzadeh, S.; Dauth, M.; Baer, R.; Kümmel, S.; Neaton, J. B.; Zojer, E.; Kronik, L. *J. Chem. Theory Comput.* **2014**, *10*, 1934−1952.
(77) Karolewski, A.; Stein, T.; Baer, R.; Kümmel, S. *J. Chem. Phys.* **2011**, *134*, 151101.
(78) Foster, M. E.; Wong, B. M. *J. Chem. Theory Comput.* **2012**, *8*, 2682−2687.
(79) Srebro, M.; Autschbach, J. *J. Chem. Theory Comput.* **2012**, *8*, 245−256.
(80) Srebro, M.; Autschbach, J. *J. Phys. Chem. Lett.* **2012**, *3*, 576−581.
(81) Minami, T.; Ito, S.; Nakano, M. *Int. J. Quantum Chem.* **2013**, *113*, 252−256.
(82) Autschbach, J.; Srebro, M. *Acc. Chem. Res.* **2014**, *47*, 2592−2602.
(83) Tamblyn, I.; Refaely-Abramson, S.; Neaton, J. B.; Kronik, L. *J. Chem. Theory Comput.* **2014**, *5*, 2734−2741.
(84) Refaely-Abramson, S.; Sharifzadeh, S.; Govind, N.; Autschbach, J.; Neaton, J. B.; Baer, R.; Kronik, L. *Phys. Rev. Lett.* **2012**, *109*, 226405.
(85) Chiba, M.; Tsuneda, T.; Hirao, K. *J. Chem. Phys.* **2006**, *124*, 144106.
(86) Becke, A. D. *Phys. Rev. A* **1988**, *38*, 3098−3100.
(87) Lee, C.; Yang, W. *Phys. Rev. B* **1988**, *37*, 785−789.
(88) Miehlich, B.; Savin, A.; Stoll, H.; Preuss, H. *Chem. Phys. Lett.* **1989**, *157*, 200−206.
(89) Becke, A. D. *J. Chem. Phys.* **1993**, *98*, 5648−5652.
(90) Neubauer, A.; Grell, G.; Friedrich, A.; Bokarev, S. I.; Schwarzbach, P.; Gärtner, F.; Surkus, A.-E.; Junge, H.; Beller, M.; Kühn, O.; Lochbrunner, S. *J. Phys. Chem. Lett.* **2014**, *5*, 1355−1360.
(91) Tomasi, J.; Mennucci, B.; Cammi, R. *Chem. Rev.* **2005**, *105*, 2999−3093.
(92) Bokarev, S. I.; Hollmann, D.; Pazidis, A.; Neubauer, A.; Radnik, J.; Kühn, O.; Lochbrunner, S.; Junge, H.; Beller, M.; Brückner, A. *Phys. Chem. Chem. Phys.* **2014**, *16*, 4789−4796.
(93) Salzner, U.; Aydin, A. *J. Chem. Theory Comput.* **2011**, 2568−2583.
(94) Zheng, S.; Geva, E.; Dunietz, B. D. *J. Chem. Theory Comput.* **2013**, *9*, 1125−1131.
(95) Refaely-Abramson, S.; Sharifzadeh, S.; Jain, M.; Baer, R.; Neaton, J. B.; Kronik, L. *Phys. Rev. B* **2013**, *88*, 081204.

DOI: 10.1021/acs.jctc.5b00068
J. Chem. Theory Comput. XXXX, XXX, XXX−XXX

(96) Phillips, H.; Zheng, Z.; Geva, E.; Dunietz, B. D. *Org. Electronics* **2014**, *15*, 1509−1520.
(97) de Queiroz, T. B.; Kümmel, S. *J. Chem. Phys.* **2014**, *141*, 084303.
(98) Janak, J. *Phys. Rev. B* **1978**, *18*, 7165−7168.
(99) Chen, J.-H.; He, L.-M.; Wang, R. L. *J. Phys. Chem. A* **2013**, *117*, 5132−5139.
(100) Bauernschmitt, R.; Ahlrichs, R. *Chem. Phys. Lett.* **1996**, *256*, 454−464.
(101) Čížek, J. *J. Chem. Phys.* **1967**, *47*, 3976.
(102) Casida, M. E.; Gutierrez, F.; Guan, J.; Gadea, F.-X.; Salahub, D. *J. Chem. Phys.* **2000**, *113*, 7062.

DOI: 10.1021/acs.jctc.5b00068
J. Chem. Theory Comput. XXXX, XXX, XXX−XXX